Journal of Sound and Vibration (1998) **217**(5), 927–944
Article No. sv981803

THREE-DIMENSIONAL VIBRATIONS OF THICK, LINEARLY TAPERED, ANNULAR PLATES

J.-H. KANG
School of Constructional and Environmental System Engineering, Kyongju University, Kyongju 780-712, *South Korea*

AND

A. W. LEISSA
Applied Mechanics Program, The Ohio State University, Columbus, OH 43210-1181, *U.S.A.*

(*Received* 2 *March* 1998, *and in final form* 18 *June* 1998)

The Ritz method is applied in a three-dimensional (3-D) analysis to obtain accurate frequencies for thick, linearly tapered, annular plates. The method is formulated for annular plates having any combination of free or fixed boundaries at both inner and outer edges. Admissible functions for the three displacement components are chosen as trigonometric functions in the circumferential co-ordinate, and algebraic polynomials in the radial and thickness co-ordinates. Upper bound convergence of the non-dimensional frequencies to the exact values within at least four significant figures is demonstrated. Comparisons of results for annular plates with linearly varying thickness are made with ones obtained by others using 2-D classical thin plate theory. Extensive and accurate (four significant figures) frequencies are presented for completely free, thick, linearly tapered annular plates having ratios of average plate thickness to difference between outer radius (a) and inner radius (b) ratios (h_m/L) of 0·1 and 0·2 for $b/L = 0{\cdot}2$ and 0·5. All 3-D modes are included in the analyses; e.g., flexural, thickness-shear, in-plane stretching, and torsional. Because frequency data given is exact to at least four digits, it is benchmark data against which the results from other methods (e.g., 2-D thick plate theory, finite element methods) and may be compared. Throughout this work, Poisson's ratio ν is fixed at 0·3 for numerical calculations.

1. INTRODUCTION

Most of the thick circular and annular plate vibration analyses have been performed with two-dimensional (2-D), sixth order plate theory, usually of the type ascribed to Mindlin [1]. Such solutions are generally valid for the lower frequency, flexural modes of moderately thick plates. However, in recent years considerable attention has been given to solutions for plates of constant thickness obtained from the exact, three-dimensional (3-D) theory of elasticity [2–9], which are valid for arbitrary thickness. In such cases the terminology "circular and

0022–460X/98/450927 + 18 $30.00/0

annular plates'' may lose their meaning, especially as the plates become very thick, and terms such as ''solid and hollow cylinders'' better describe the problem. As computers and analytical procedures become more efficient, three-dimensional solutions will definitely become increasingly important in the future, not only for obtaining accurate frequencies and mode shapes, but for verifying the accuracies of two-dimensional plate theories.

In the case of plates with variable thickness, the governing differential equation of motion of 2-D theory is found to have variable coefficients, and this fact increases the difficulty of solution. Nevertheless, considerable attention has been paid to variable thickness plates in recent years. As regards circular and annular plates of variable thickness, a great deal of information is available for various types of thickness variations and conditions at the boundary of the plates. Leissa's book [10] and series of review articles [11–13] on plate vibrations are reasonably thorough sources of information for the periods preceding 1966 [10], and from 1973 to 1985 [11–13].

Early 2-D investigations of vibrations of circular and annular plates with variable thickness were made by Conway [14, 15], Kovalenko [16], Kazantseva [17], and Ehrich [18] using classical, thin plate theory. Kovalenko's [16] primary work was a direct attack upon the differential equation by assuming a series form of solution. Boundary conditions led to an infinite characteristic determinant, which was truncated for an approximate solution. Numerical results were not given for completely free boundary conditions, but for edges free on the outside and clamped on the inside.

Sony and Amba Rao [19] conducted a study of the free axisymmetric vibrations of orthotropic circular plates with linear variation in thickness. The governing differential equations were derived on the basis of Mindlin plate theory. The Chebyshev collocation technique was adopted to solve the differential equations.

Annular Mindlin plates of varying thickness were also considered by Irie *et al*. [20]. Gupta and Lal [21] analyzed the axisymmetric vibrations of polar orthotropic Mindlin annular plates of variable thickness using a Chebyshev collocation technique. Singh and Goel [22], and Singh and Tyagi [23] studied elliptic and circular plates using the Ritz method and obtained a sequence of approximations. In another series of papers Singh and Chakraverty [24–29] used characteristic orthogonal polynomials with the same method to obtain the frequencies and mode shapes of circular and elliptic plates with constant and variable thickness under different boundary conditions.

Recently, employing the Ritz method, Singh and Saxena [30] studied the axisymmetric transverse vibration of a circular plate with two different linear variations in thickness; one in the central core and the other in the outer annular region. The boundary was taken to be either clamped or simply supported. Gutierrez *et al*. [31] investigated the vibration and buckling of circular plates of thickness varying according to the functional relation $h_0[1 + \gamma(\bar{r}/a)^n]$, where n is a positive integer, using the classical Ritz method.

However, none of the above references for variable thickness plates determined frequencies by 3-D analysis. The primary objective of the present work is to present truly accurate values of the free-vibration frequencies of thick, linearly tapered, annular plates. Besides presenting the method of analysis and establishing its accuracy by means of convergence studies, comparisons are made with other 2-D results. The accurate 3-D results presented here serve as benchmarks against which other approximate methods (e.g., finite element, finite difference methods) and 2-D plate theories, first order and higher order, may be tested.

2. METHOD OF ANALYSIS

A representative annular plate with thickness (h) varying linearly along the radial direction, with inner radius b, outer radius a, inner edge thickness h_i, and outer edge thickness h_o, is shown in Figure 1.

The local co-ordinate system (s, θ, z), also shown in the figure, is used in the analysis. The radial (s) and thickness (z) co-ordinates are measured normally from the inner edge and the mid-plane of the annular plate, respectively, and θ is the circumferential angle. The radial co-ordinate could equally well originate at the center of the plate, but is used in the present manner to be consistent with a more general method of analysis applicable to thick shells having variable curvature and thickness [32].

To analyze the free vibrations of the annular plate the kinetic energy (T) and strain (potential) energy (V) will be developed in terms of three displacement components u, v, and w, which are taken positive in the directions of increasing s, θ, and z (see Figure 1).

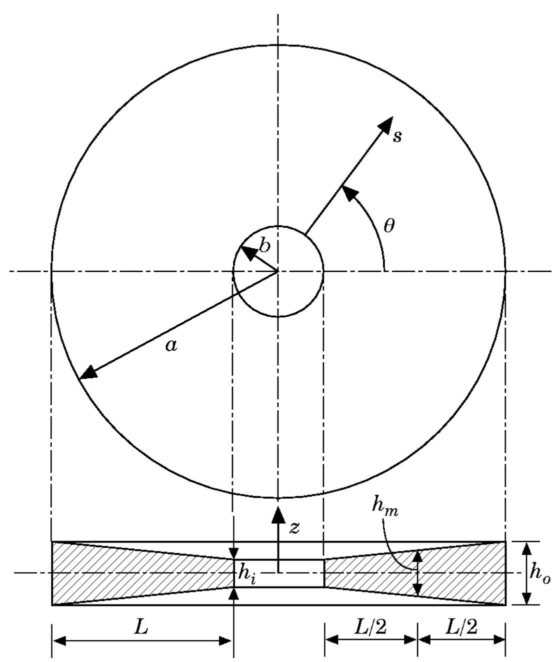

Figure 1. Cross-section of a thick, linearly tapered annular plate with local co-ordinate system (s, θ, z).

The kinetic energy is simply

$$T = \tfrac{1}{2}\int_{\Omega} \rho(\dot{u}^2 + \dot{v}^2 + \dot{w}^2)(s+b)\,\mathrm{d}s\,\mathrm{d}\theta\,\mathrm{d}z, \tag{1}$$

where ρ is mass density, the dots ($\dot{}$) denote time derivatives, and the integration is carried out over the domain (Ω) of the annular plate.

The strain (potential) energy of deformation is expressed in terms of the stresses (σ_{ij}) and strains (ϵ_{ij}) as

$$V = \tfrac{1}{2}\int_{\Omega} (\sigma_{ss}\epsilon_{ss} + \sigma_{\theta\theta}\epsilon_{\theta\theta} + \sigma_{zz}\epsilon_{zz} + \sigma_{s\theta}\epsilon_{s\theta} + \sigma_{sz}\epsilon_{sz} + \sigma_{\theta z}\epsilon_{\theta z})(s+b)\,\mathrm{d}s\,\mathrm{d}\theta\,\mathrm{d}z. \tag{2}$$

The well-known stress–strain equations of isotropic, linear elasticity are:

$$\sigma_{ii} = \lambda(\epsilon_{ss} + \epsilon_{zz} + \epsilon_{\theta\theta}) + 2G\epsilon_{ii}, \qquad \sigma_{ij} = G\epsilon_{ij}(i \neq j), \tag{3}$$

where λ and G are the Lamé parameters (G. Lamé 1852), expressed in terms of Young's modulus (E) and Poisson's ratio (ν) for an isotropic solid as

$$\lambda = E\nu/(1+\nu)(1-2\nu), \qquad G = E/2(1+\nu). \tag{4}$$

The three-dimensional strains are found to be related to the displacements by

$$\epsilon_{ss} = u_{,s}, \qquad \epsilon_{\theta\theta} = [1/(s+b)](u + v_{,\theta}), \qquad \epsilon_{zz} = w_{,z}, \tag{5a–c}$$

$$\epsilon_{s\theta} = [1/(s+b)][u_{,\theta} - v + (s+b)v_{,s}], \qquad \epsilon_{sz} = u_{,z} + w_{,s},$$

$$\epsilon_{\theta z} = [1/(s+b)][(s+b)v_{,z} + w_{,\theta}], \tag{5d–f}$$

where subscripted symbols following commas denote differentiations.

Substituting equations (3) and (5) into equation (2) results in

$$V = \tfrac{1}{2}\int_{\Omega} [\lambda(\epsilon_{ss} + \epsilon_{\theta\theta} + \epsilon_{zz})^2 + G\{2(\epsilon_{ss}^2 + \epsilon_{\theta\theta}^2 + \epsilon_{zz}^2)$$

$$+ \epsilon_{s\theta}^2 + \epsilon_{sz}^2 + \epsilon_{\theta z}^2\}](s+b)\,\mathrm{d}s\,\mathrm{d}\theta\,\mathrm{d}z. \tag{6}$$

For convenience, the s and z co-ordinates are made dimensionless,

$$\psi \equiv s/L, \qquad \zeta \equiv z/h_m, \tag{7}$$

where L is the radial width of the plate, $a - b$, and h_m is the average plate thickness, defined by $h_m \equiv (h_i + h_o)/2$.

For the free, undamped vibration, the time (t) response of the three displacements is sinusoidal and, moreover, the circular symmetry of the plate allows the displacements to be expressed by

$$u(\psi, \theta, \zeta, t) = U(\psi, \zeta)\cos n\theta \sin(\omega t + \alpha), \tag{8a}$$

$$v(\psi, \theta, \zeta, t) = V(\psi, \zeta)\sin n\theta \sin(\omega t + \alpha), \tag{8b}$$

$$w(\psi, \theta, \zeta, t) = W(\psi, \zeta)\cos n\theta \sin(\omega t + \alpha), \tag{8c}$$

where U, V, and W are displacement functions of ψ and ζ, ω is a natural frequency, α is an arbitrary phase angle determined by the initial conditions, and $n = 0, 1, 2, \ldots, \infty$. By substituting equations (8) into the three partial differential equations of motion for the body, expressed in cylindrical co-ordinates, one may verify that these are proper assumed forms for the displacements, and that θ and t are thereby uncoupled from ψ and ζ.

A complementary set of functions may also be used for equations (8) replacing $\cos n\theta$ by $\sin n\theta$, and conversely. This gives the same vibratory mode shapes rotated by $\pi/2n$ in θ, and the same frequencies, except for $n = 0$. For $n = 0$, equations (8) yield the axisymmetric modes which involve only u and w (for example, longitudinal and/or radial extension). However, the complementary set for $n = 0$ yields the torsional modes, which involve only v, uncoupled from u and w. Thus, for the annular cross-section, there is no warping of the cross-section during torsional vibration.

Using algebraic polynomials which are mathematically complete, displacement functions U, V, and W in equations (8) which are capable of satisfying any geometrical boundary conditions may be represented by

$$U = \eta \sum_{i=0}^{I} \sum_{j=0}^{J} A_{ij} \psi^i \zeta^j, \qquad V = \eta \sum_{k=0}^{K} \sum_{l=0}^{L} B_{kl} \psi^k \zeta^l, \qquad W = \eta \sum_{m=0}^{M} \sum_{n=0}^{N} C_{mn} \psi^m \zeta^n, \tag{9a–c}$$

where i, j, k, l, m, and n are integers; I, J, K, L, M, and N are the highest degrees of the polynomial terms; A_{ij}, B_{kl}, and C_{mn} are arbitrary coefficients; and η depends upon the boundary conditions to be enforced. For example: (1) completely free: $\eta = 1$; (2) inner edge fixed, outer edge free: $\eta = \psi$; (3) outer edge fixed, inner edge free: $\eta = \psi - 1$; (4) both inner and outer edges fixed: $\eta = \psi(\psi - 1)$.

The η functions shown above impose only the necessary geometric constraints at the boundaries, which are required when using the Ritz method, and ignore boundary conditions involving stress. Together with the algebraic polynomials, equations (9), they form mathematically complete sets (reference [33], pp. 266–268) that are capable of representing the free vibration mode shapes of an annular plate to any degree of accuracy desired.

The Ritz method uses the maximum energy functionals for the vibrating system. The maximum potential energy (V_{max}) during a vibratory cycle is due to the strain energy of deformation. Using equations (6)–(8) it becomes

$$V_{max} = \frac{LG}{2} \int_0^1 \int_{-\delta(\psi)/2}^{\delta(\psi)/2} \left[\left\{ \frac{\lambda}{G} (K_1 + K_2 + K_3)^2 + 2(K_1^2 + K_2^2 + K_3^2) + K_4^2 \right\} \Gamma_1 + (K_5^2 + K_6^2) \Gamma_2 \right] r^* \, \mathrm{d}\zeta \, \mathrm{d}\psi, \tag{10}$$

where

$$K_1 \equiv (U + nV)/r^*, \qquad K_2 \equiv (h_m/L)U_{,\psi}, \qquad K_3 \equiv W_{,\zeta}, \qquad K_4 \equiv U_{,\zeta} + (h_m/L)W_{,\psi},$$

$$K_5 \equiv V_{,\zeta} - nW/r^*, \qquad K_6 \equiv (nU + V)/r^* - (h_m/L)V_{,\psi}, \tag{11}$$

and r^* is defined by

$$r^* \equiv (s + b)/h_m = (\psi + b/L)L/h_m, \tag{12}$$

and $\delta(\psi)$ is the non-dimensional thickness, defined by

$$\delta(\psi) \equiv h(s)/h_m = [2/(1 + h^*)][(1 - h^*)\psi + h^*], \tag{13}$$

where h^* is the taper ratio of h_i/h_o, and Γ_1 and Γ_2 are constants defined by

$$\Gamma_1 \equiv \int_0^{2\pi} \cos^2 n\theta \, \mathrm{d}\theta = \begin{Bmatrix} 2\pi, & \text{if } n = 0 \\ \pi, & \text{if } n \geqslant 1 \end{Bmatrix}, \qquad \Gamma_2 \equiv \int_0^{2\pi} \sin^2 n\theta \, \mathrm{d}\theta = \begin{Bmatrix} 0, & \text{if } n = 0 \\ \pi, & \text{if } n \geqslant 1 \end{Bmatrix}. \tag{14}$$

It is known that λ and G have the same dimensions as E from equations (4). The non-dimensional constant λ/G in equation (10) involves only ν; i.e., $\lambda/G = 2\nu/(1 - 2\nu)$.

The maximum kinetic energy during a vibratory cycle is

$$T_{max} = \frac{\rho L h_m^2 \omega^2}{2} \int_0^1 \int_{-\delta(\psi)/2}^{\delta(\psi)/2} [(U^2 + W^2)\Gamma_1 + V^2 \Gamma_2] r^* \, \mathrm{d}\zeta \, \mathrm{d}\psi. \tag{15}$$

The eigenvalue problem for finding natural frequencies and mode shapes is determined from the Ritz minimizing equations. For this present problem, these are

$$\frac{\partial(V_{max} - T_{max})}{\partial A_{ij}} = 0, \quad \begin{pmatrix} i = 0, 1, 2, \ldots, I \\ j = 0, 1, 2, \ldots, J \end{pmatrix}, \tag{16a}$$

$$\frac{\partial(V_{max} - T_{max})}{\partial B_{kl}} = 0, \quad \begin{pmatrix} k = 0, 1, 2, \ldots, K \\ l = 0, 1, 2, \ldots, L \end{pmatrix}, \tag{16b}$$

$$\frac{\partial(V_{max} - T_{max})}{\partial C_{mn}} = 0, \quad \begin{pmatrix} m = 0, 1, 2, \ldots, M \\ n = 0, 1, 2, \ldots, N \end{pmatrix}. \tag{16c}$$

The minimizing conditions of equations (16) produce a set of algebraic equations (or Ritz system) consisting of $[(I+1)(J+1)+(K+1)(L+1)+(M+1)(N+1)]$ linear, homogeneous, algebraic equations with the same number of unknowns A_{ij}, B_{kl}, and C_{mn}. The equations can be written in the form

$$(\mathbf{K}-\Lambda\mathbf{M})\mathbf{x}=\mathbf{0} \qquad \text{or} \qquad (\mathbf{K}\mathbf{M}^{-1}-\Lambda\mathbf{I})\mathbf{x}=\mathbf{0}, \tag{17}$$

where **K** and **M** are stiffness and mass matrices resulting from the maximum strain energy (V_{max}) and the maximum kinetic energy (T_{max}), respectively, and Λ is an eigenvalue of the vibrating system, expressed as the square of non-dimensional frequency, $\omega^2 h_m^2 \rho/G$, and the vector **x** takes the form

$$\mathbf{x}=(A_{00}, A_{01}, \ldots, A_{IJ}; B_{00}, B_{01}, \ldots, B_{KL}; C_{00}, C_{01}, \ldots, C_{MN})^{\mathrm{T}}. \tag{18}$$

TABLE 1

Convergence of frequencies $\omega a\sqrt{\rho/G}$ of a completely free, annular plate with linearly varying thickness along the radial direction for the five lowest modes for $n=2$ with $h_i/h_o=1/3$, $b/L=0{\cdot}2$, $h_m/L=0{\cdot}2$ and $\nu=0{\cdot}3$

TZ	***TS***	***DET***	1	2	3	4	5
2	2	12	0·5029	1·847	3·587	4·127	8·684
2	4	24	0·4182	1·707	2·540	4·058	5·587
2	6	36	0·4166	1·692	2·514	4·050	5·066
2	8	48	0·4165	1·688	2·512	4·049	4·999
2	10	60	0·4165	1·687	2·512	4·049	4·995
3	2	18	0·4678	1·843	3·520	4·126	8·616
3	4	36	0·4064	1·704	2·355	4·057	5·343
3	6	54	0·4052	1·690	2·355	4·050	4·748
3	8	72	0·4051	1·686	2·334	**4·048**	4·692
3	10	90	0·4051	**1·685**	2·334	4·048	4·690
4	2	24	0·4602	1·842	3·450	4·124	8·610
4	4	48	0·4033	1·704	2·329	4·057	5·290
4	6	72	0·4022	1·690	2·310	4·050	4·676
4	8	96	0·4022	1·686	2·309	4·048	4·622
4	10	120	**0·4021**	1·685	2·309	4·048	4·620
5	2	30	0·4602	1·841	3·445	4·124	8·604
5	4	60	0·4033	1·704	2·328	4·057	5·287
5	6	90	0·4022	1·690	2·309	4·050	4·673
5	8	120	0·4022	1·686	**2·308**	4·048	4·620
5	10	150	0·4021	1·685	2·308	4·048	**4·619**
6	2	36	0·4598	1·841	3·435	4·124	8·604
6	4	72	0·4031	1·704	2·328	4·057	5·274
6	6	108	0·4022	1·690	2·309	4·050	4·670
6	8	144	0·4021	1·686	2·308	4·048	4·620
6	9	162	0·4021	1·686	2·308	4·048	4·619

Notes: ***TZ*** = total number of natural polynomial terms used in the z or ζ direction; ***TS*** = total number of natural polynomial terms used in the s or ψ direction: ***DET*** = determinant order.

Equation (17) represents the eigenvalue problem. For a non-trivial solution, the determinant of the coefficient matrix is set to zero; that is to say $|\mathbf{K} - \Lambda\mathbf{M}| = 0$ or $|\mathbf{K}\mathbf{M}^{-1} - \Lambda\mathbf{I}| = 0$ where $\mathbf{I}$ is an identity matrix and $\mathbf{M}^{-1}$ is the inverse of $\mathbf{M}$. The roots of the determinant are the eigenvalues. Substituting each eigenvalue back into the equations generating the eigenvalue determinant yields the corresponding eigenvector, and substituting the eigenvector into the displacement functions will give the mode shape for each eigenvalue.

TABLE 2

Non-dimensional frequencies $\omega L\sqrt{\rho/G}$ *of completely free, annular plates with linearly varying thickness along the radial direction for* $b/L = 0{\cdot}2$, $h_m/L = 0{\cdot}1$ *and* $\nu = 0{\cdot}3$

		h_i/h_o				
n	Mode	0	1/3	1	3	∞
0(T)	1	6·118	5·558	5·181	4·997	5·375
	2	9·768	8·949	8·640	8·512	9·027
	3	13·38	12·40	12·16	12·06	12·66
	4	17·01	15·95	15·76	15·68	16·34
	5	20·66	19·57	19·41	19·34	20·04
0(A)	1	(2) 0·3875	(2) 0·3198	(2) 0·3438	(2) 0·4334	(2) 0·6510
	2	1·657	1·505	1·557	1·592	1·763
	3	2·449	2·799	3·152	3·501	3·323
	4	3·246	3·427	3·573	3·568	4·104
	5	5·217	5·981	6·241	6·039	5·277
1	1	(4) 0·6589	(4) 0·6966	(4) 0·7851	(5) 0·8666	(5) 1·092
	2	1·805	1·903	2·113	2·206	2·321
	3	2·728	2·739	2·776	2·890	3·271
	4	3·360	3·739	4·014	4·017	3·810
	5	5·315	6·220	6·384	6·399	5·630
2	1	(1) 0·2368	(1) 0·2104	(1) 0·2085	(1) 0·2550	(1) 0·4005
	2	1·211	1·298	1·339	1·343	1·502
	3	1·338	1·686	1·995	2·310	2·620
	4	2·219	2·742	3·026	3·046	2·973
	5	3·691	4·049	4·080	4·192	4·667
3	1	(3) 0·6430	(3) 0·5562	(3) 0·4937	(3) 0·4919	(3) 0·6735
	2	1·918	2·026	2·005	1·913	1·957
	3	2·731	3·129	3·551	3·902	3·607
	4	2·845	3·735	3·987	4·093	4·862
	5	4·220	5·703	5·786	5·950	5·536
4	1	(5) 1·190	(5) 1·018	(5) 0·8572	(4) 0·7496	(4) 0·8893
	2	2·773	2·851	2·734	2·502	2·366
	3	3·650	4·268	4·684	4·762	4·200
	4	3·929	4·809	4·980	5·288	6·296
	5	4·925	6·999	7·428	7·359	6·311

Notes: $T \sim$ torsional mode; $A \sim$ axisymmetric mode; numbers in parentheses identify frequency sequences.

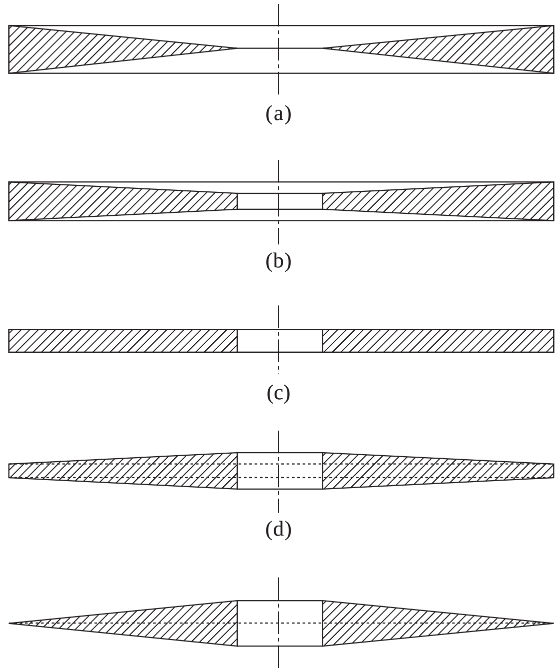

Figure 2. Cross-sections of annular plates with $b/L = 0{\cdot}2$ and $h_m/L = 0{\cdot}1$: (a) $h_i/h_o = 0$; (b) $h_i/h_o = 1/3$; (c) $h_i/h_o = 1$; (d) $h_i/h_o = 3$; (e) $h_i/h_o = \infty$.

As it is well-known, frequencies by the Ritz method converge in the manner of upper bounds to the exact values. These upper bounds are improved by increasing the numbers of polynomial terms in equations (9). Since the algebraic polynomials of equations (9) form sets which are mathematically complete, as sufficient numbers of terms are taken, monotonic convergence to the exact frequencies is guaranteed.

3. CONVERGENCE STUDIES

A convergence study is based upon the fact that all the frequencies obtained by the Ritz method should converge to their exact values in an upper bound manner. If the results do not converge properly, or converge too slowly, it is likely that the assumed displacements may be poor ones, or be missing some functions from a minimal complete set of polynomials.

In Table 1, the results of a convergence study of nondimensional frequencies $\omega a\sqrt{\rho/G}$ for $n = 2$ are shown for the annular plate with linearly varying thickness in the radial direction for $h_i/h_o = 1/3$, $b/L = h_m/L = 0{\cdot}2$, and $\nu = 0{\cdot}3$. This annular plate is a thick one, for which classical plate theory would be inappropriate.

To make the study of convergence less complicated, equal numbers of polynomial terms were taken in both the s or ψ-co-ordinate (i.e., $I = K = M$) and z or ζ-co-ordinate (i.e., $J = L = N$), although some computational optimization could be obtained for some configurations and some mode shapes by using unequal numbers of polynomial terms.

The symbols $\boldsymbol{TZ}$ and $\boldsymbol{TS}$ in the table indicate the total numbers of polynomial terms used in the z (or ζ) and s (or ψ) directions, respectively. Note that the determinant order $\boldsymbol{DET}$ is related to $\boldsymbol{TZ}$ and $\boldsymbol{TS}$ as follows:

$$\boldsymbol{DET} = \left\{\begin{array}{ll} \boldsymbol{TZ} \times \boldsymbol{TS} & \text{for torsional modes } (n=0) \\ 2 \times \boldsymbol{TZ} \times \boldsymbol{TS} & \text{for axisymmetric modes } (n=0) \\ 3 \times \boldsymbol{TZ} \times \boldsymbol{TS} & \text{for general modes } (n \geqslant 1) \end{array}\right\}. \tag{19}$$

TABLE 3

Non-dimensional frequencies $\omega L\sqrt{\rho/G}$ of completely free, annular plates with linearly varying thickness along the radial direction for $b/L = 0{\cdot}2$, $h_m/L = 0{\cdot}2$ and $\nu = 0{\cdot}3$

		h_i/h_o				
n	Mode	0	1/3	1	3	∞
0(T)	1	6·088	5·551	5·181	4·991	5·348
	2	9·719	8·938	8·640	8·502	8·981
	3	10·82	12·39	12·16	12·05	12·60
	4	13·31	13·78	15·76	15·51	12·82
	5	16·73	15·93	18·85	15·66	16·25
0(A)	1	(2) 0·7306	(2) 0·6173	(2) 0·6687	(2) 0·8440	(2) 1·253
	2	2·448	2·717	2·804	2·878	3·204
	3	3·000	2·798	3·150	3·559	4·077
	4	5·548	5·644	5·829	5·782	5·703
	5	8·376	8·242	8·047	8·120	8·553
1	1	(4) 1·195	(4) 1·286	(4) 1·454	(5) 1·611	(5) 2·016
	2	2·727	2·738	2·776	2·888	3·263
	3	3·244	3·332	3·597	3·718	3·945
	4	5·717	6·062	6·340	6·300	6·131
	5	6·978	6·537	6·368	6·577	7·284
2	1	(1) 0·4392	(1) 0·4021	(1) 0·4062	(1) 0·4958	(1) 0·7641
	2	(5) 1·336	(5) 1·685	1·995	2·308	2·610
	3	2·135	2·308	2·416	2·459	2·765
	4	3·925	4·048	4·078	4·189	4·654
	5	4·038	4·619	5·001	5·080	5·131
3	1	(3) 1·140	(3) 1·027	(3) 0·9422	(3) 0·9540	(3) 1·295
	2	2·720	3·124	3·480	3·408	3·560
	3	3·273	3·445	3·551	4·090	4·844
	4	4·954	5·698	5·783	5·946	6·147
	5	5·630	6·023	6·356	6·330	6·534
4	1	2·002	1·805	(5) 1·592	(4) 1·437	(4) 1·707
	2	3·907	4·260	4·577	4·351	4·278
	3	4·530	4·638	4·684	5·284	6·284
	4	6·271	7·322	7·421	7·533	7·095
	5	7·241	7·419	7·671	7·605	8·333

Notes: $T \sim$ torsional mode; $A \sim$ axisymmetric mode; numbers in parentheses identify frequency sequences.

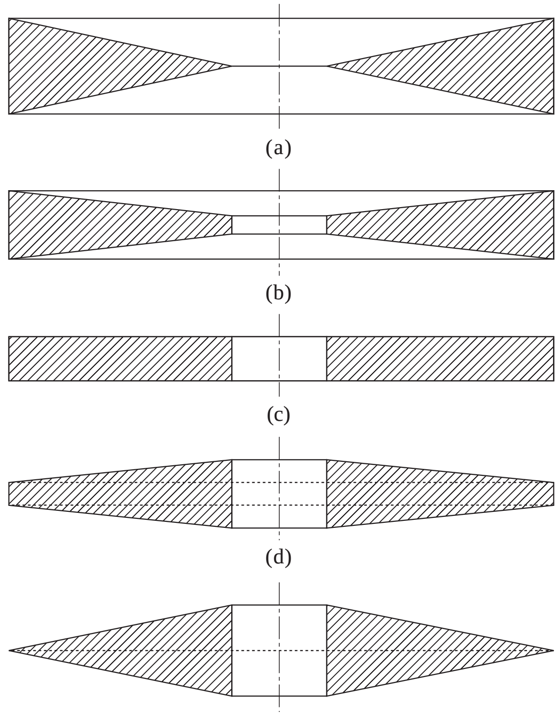

Figure 3. Cross-sections of annular plates with $b/L = 0{\cdot}2$ and $h_m/L = 0{\cdot}2$: (a) $h_i/h_o = 0$; (b) $h_i/h_o = 1/3$; (c) $h_i/h_o = 1$; (d) $h_i/h_o = 3$; (e) $h_i/h_o = \infty$.

In the table, there are five columns of data corresponding to the five lowest frequencies. The frequencies in bold and underlined indicate the best convergent values in each column with the smallest determinant size. The zero frequencies corresponding to the rigid body modes have been removed. The values of ***TZ*** and ***TS*** begin with 2, increasing ***TS*** by 2 up to 10, and ***TZ*** by 1 up to 6. When ***TZ*** is 6, ***TS*** is taken as 9 instead of 10, since it would require a tremendous computer time and memory to evaluate the stiffness and mass matrices. Frequencies in the table are given to four digits.

It is interesting to note that the frequencies seen in Table 1 for the first, second and fourth modes are reasonably accurate even when only two polynomial terms are taken through the thickness (***TZ*** $= 2$), provided enough terms are used in the radial direction (***TS*** $\geqslant 8$). However, the third and fifth frequencies are quite inaccurate ***TZ*** $= 2$, being 8·8 and 8·1% too high, respectively. This low degree solution corresponds to the Mindlin thick plate theory, which permits no variation in z for the w displacement, and restricts u and v to vary linearly with z.

One may also note that the mode shapes uncouple into ones which are either symmetric or antisymmetric with respect to the mid-plane ($z = 0$) of the plate. The lower frequency modes described in Table 1 are all antisymmetric, involving predominantly bending and thickness-shear. The symmetric modes (e.g., radial and axial extension) are higher frequency ones.

Additional convergence studies were also made for other circumferential numbers ($n = 0$, torsional and axisymmetric; and $n = 1$) by Kang [32]. They showed similar rates of convergence.

4. NUMERICAL RESULTS AND DISCUSSION

Tables 2–5 present accurate (four significant figure) nondimensional frequencies $\omega a\sqrt{\rho/G}$ of completely free, thick, linearly tapered, annular plates. Figures 2–5

TABLE 4

Non-dimensional frequencies $\omega L\sqrt{\rho/G}$ of completely free, annular plates with linearly varying thickness along the radial direction for $b/L = 0{\cdot}5$, $h_m/L = 0{\cdot}1$ and $\nu = 0{\cdot}3$

		h_i/h_o				
n	Mode	0	1/3	1	3	∞
0(T)	1	6·912	6·059	5·604	5·461	5·990
	2	11·41	10·28	9·971	9·890	10·62
	3	15·97	14·73	14·52	14·46	15·29
	4	20·57	19·30	19·14	19·09	19·98
	5	25·20	23·93	23·80	23·75	24·68
0(A)	1	(2) 0·3497	(2) 0·2665	(2) 0·2713	(2) 0·3494	(2) 0·5363
	2	1·932	1·694	1·709	1·711	1·919
	3	2·181	2·405	2·629	2·864	3·113
	4	3·921	4·092	4·221	4·094	3·889
	5	6·392	7·301	7·580	7·294	6·354
1	1	(4) 0·5403	(4) 0·4835	(4) 0·5564	(5) 0·6836	(5) 0·9371
	2	2·000	1·827	1·898	1·937	2·133
	3	2·704	2·756	2·840	2·997	3·354
	4	3·975	4·193	4·351	4·238	4·019
	5	6·438	6·954	6·680	6·661	6·447
2	1	(1) 0·1762	(1) 0·1551	(1) 0·1545	(1) 0·1920	(1) 0·2907
	2	0·9149	0·9044	1·019	1·134	1·406
	3	1·004	1·249	1·421	1·542	1·594
	4	2·200	2·194	2·401	2·528	2·716
	5	4·052	4·050	4·096	4·260	4·437
3	1	(3) 0·4861	(3) 0·4221	(3) 0·3896	(3) 0·4240	(3) 0·6100
	2	1·348	1·436	1·566	1·631	1·846
	3	2·282	2·700	3·051	3·283	3·388
	4	2·516	2·741	3·105	3·361	3·567
	5	4·397	4·955	5·338	5·381	5·130
4	1	(5) 0·9141	(5) 0·7884	(5) 0·6900	(4) 0·6643	(4) 0·8692
	2	1·828	2·074	2·196	2·186	2·303
	3	2·931	3·433	3·943	4·112	4·048
	4	3·533	4·003	4·472	4·998	5·494
	5	4·757	5·574	6·136	6·292	5·960

Notes: $T \sim$ torsional mode; $A \sim$ axisymmetric mode; numbers in parentheses identify frequency sequences.

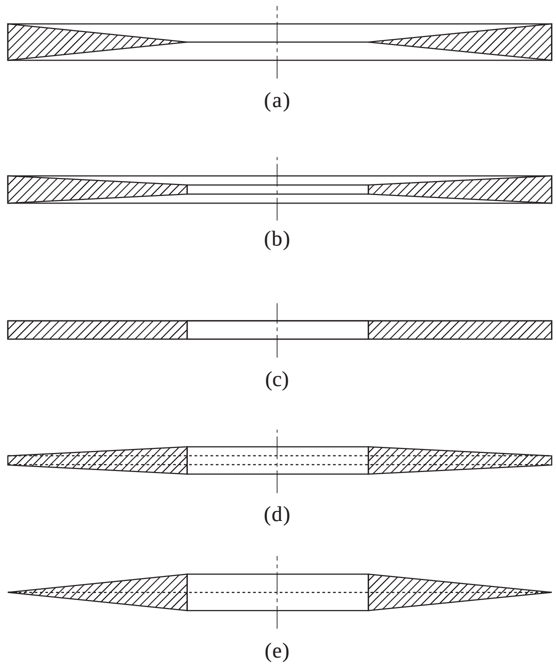

Figure 4. Cross-sections of annular plates with $b/L = 0{\cdot}5$ and $h_m/L = 0{\cdot}1$: (a) $h_i/h_o = 0$; (b) $h_i/h_o = 1/3$; (c) $h_i/h_o = 1$; (d) $h_i/h_o = 3$; (e) $h_i/h_o = \infty$.

show the configurations corresponding to Tables 2–5, respectively. Thirty frequencies are given for each configuration, which arise from six circumferential mode numbers (n), (i.e., $n = 0(T)$, $0(A)$, 1, 2, 3, 4) and the first five modes for each value of n, where T and A indicate torsional and axisymmetric modes, respectively. Numbers in parentheses identify the first five frequencies for each configuration. The zero frequencies of rigid body modes are omitted from the tables.

It is seen that irrespective of the aspect ratio (b/L), thickness ratio (h_m/L), and the taper ratio (h_i/h_o), the fundamental, second, and third frequencies occur with mode shapes having two ($n = 2$), zero ($n = 0$, axisymmetric), and three ($n = 3$) circumferential waves, respectively. It is known that the fundamental mode is in bending with $n = 2$ for a completely free annular plate with constant thickness [10].

Table 2 shows that, for the moderately thick plate ($h_m/L = 0{\cdot}1$) having a relatively small hole ($b/L = 0{\cdot}2$, which corresponds to $b/a = 1/6$), most of the frequencies are not changed greatly by the drastic variation of inner-to-outer thickness ratio ($0 \leqslant h_i/h_o \leqslant \infty$) when the average thickness (h_m) is kept constant. However, the first two modes ($n = 2$ and $0(A)$) are notable exceptions to this, with the frequencies nearly doubling as the plate varies from having a sharp inner edge ($h_i/h_o = 0$) to having a sharp outer edge ($h_i/h_o = \infty$), as shown in Figure 2. Considering thicker plates ($h_m/L = 0{\cdot}2$, Table 3) or ones with a larger hole ($b/L = 0{\cdot}5$, Table 4), the frequencies are seen to be somewhat more greatly affected with changing h_i/h_o.

One also sees in Tables 2–5 that for a plate having a fixed average thickness (h_m) the first two frequencies are always largest when the greatest thickness is at the inner edge ($h_i/h_o = \infty$), but not necessarily for the other modes.

As expected in Tables 2–5, the torsional ($n = 0(T)$) frequencies, are much greater than the axisymmetric ($n = 0(A)$) frequencies. This is because, even for these thick plate configurations, the axisymmetric modes are predominantly bending, with the largest displacement components being normal to the plate middle surface,

TABLE 5

Non-dimensional frequencies $\omega L\sqrt{\rho/G}$ *of completely free, annular plates with linearly varying thickness along the radial direction for* $b/L = 0{\cdot}5$, $h_m/L = 0{\cdot}2$ *and* $\nu = 0{\cdot}3$

		h_i/h_o				
n	Mode	0	1/3	1	3	∞
0	1	6·879	6·051	5·604	5·454	5·960
	2	11·36	10·26	9·971	9·877	10·57
	3	13·62	14·72	14·52	14·44	14·98
	4	15·88	17·31	19·14	18·50	15·21
	5	20·45	19·28	23·56	19·06	19·87
0	1	(2) 0·6639	(2) 0·5186	(2) 0·5316	(2) 0·6838	(2) 1·034
	2	2·181	2·405	2·628	2·862	3·109
	3	3·513	3·086	3·112	3·123	3·501
	4	6·721	6·770	6·920	6·790	6·690
	5	10·116	8·970	8·614	8·783	9·948
1	1	(4) 0·9887	(4) 0·9142	(4) 1·042	(4) 1·254	1·6640
	2	2·703	2·756	2·839	2·995	3·349
	3	3·620	3·296	3·388	3·420	3·742
	4	6·796	6·908	6·676	6·650	6·808
	5	7·536	6·942	7·083	6·948	7·139
2	1	(1) 0·3332	(1) 0·3001	(1) 0·3027	(1) 0·3729	(1) 0·5517
	2	(5) 1·003	(5) 1·248	1·421	1·539	(4) 1·586
	3	1·651	1·675	1·886	2·099	2·572
	4	3·932	3·877	4·095	4·257	4·542
	5	4·050	4·049	4·145	4·274	4·747
3	1	(3) 0·8941	(3) 0·8237	(3) 0·7536	(3) 0·8237	(3) 1·164
	2	2·276	2·975	2·835	2·975	3·372
	3	2·428	3·356	3·051	3·356	3·550
	4	4·423	5·446	5·216	5·446	5·681
	5	5·680	5·781	5·620	5·781	6·404
4	1	1·621	1·450	(5) 1·310	(5) 1·283	(5) 1·6638
	2	3·291	3·646	3·862	3·901	4·164
	3	3·519	3·998	4·472	4·993	5·470
	4	5·064	5·799	6·461	6·708	6·806
	5	7·184	7·188	7·197	7·313	7·978

Notes: $T \sim$ torsional mode; $A \sim$ axisymmetric mode; numbers in parentheses identify frequency sequences.

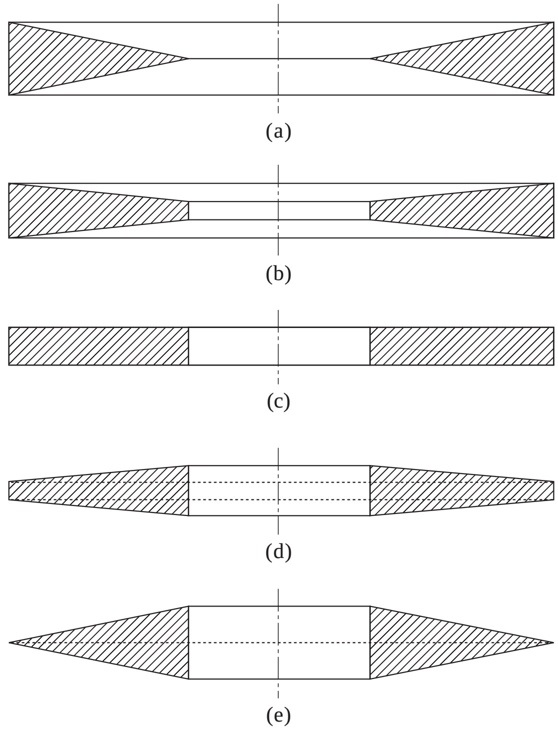

Figure 5. Cross-sections of annular plates with $b/L = 0{\cdot}5$ and $h_m/L = 0{\cdot}2$: (a) $h_i/h_o = 0$; (b) $h_i/h_o = 1/3$; (c) $h_i/h_o = 1$; (d) $h_i/h_o = 3$; (e) $h_i/h_o = \infty$.

whereas the torsional modes involve shearing, with the sole component being tangent to the plate middle surface, which entails greater stiffness than bending.

Comparing the torsional frequencies ($n = 0(T)$) between Tables 2 and 3, it is seen that, for uniform thickness ($h_i/h_o = 1$), the first four (5·181, 8·640, 12·16, 15·76) are unaffected by doubling the plate thickness. These are counter-rotating modes, where the inner portion moves oppositely to its adjacent portion, creating nodal cylindrical surfaces of no displacement between them. These frequencies are obtainable as exact solutions, where the circumferential displacement (V) varies with ψ (or s) as a Bessel function (cf. reference [34]). The same phenomenon is seen for the plates with the larger holes, comparing Tables 4 and 5. However, it is also seen that such relationships do not exist when the plate thickness is not constant ($h_i/h_o \neq 1$).

5. COMPARISONS WITH 2-D PLATE RESULTS

Ramaiah and Vijayakumar [35] made a thorough study of annular circular plates with linear thickness variations, both increasing and decreasing with the radius. They treated all nine possible combinations of clamped, simply supported, and free edge conditions using various taper ratios (h_o/h_i or h_i/h_o) and boundary radii ratios (b/a). They employed the Ritz method with nine trial functions in the radial direction, which should be sufficient to give accurate results. Their analysis is based upon the 2-D thin plate theory. Frequencies corresponding to axisymmetric modes ($n = 0$) as well as for modes with one ($n = 1$) and two ($n = 2$) nodal diameters were obtained. The non-dimensional frequency parameter used for the annular plate was given by $2(\omega a^2/h_i)\sqrt{\rho/E}$ for $h_i > h_o$ or $2(\omega a^2/h_o)\sqrt{\rho/E}$ for $h_i < h_o$.

Table 6 compares the frequencies in $2(\omega a^2/h_o)\sqrt{\rho/E}$ from the 3-D and 2-D theories for four thin annular plates with linearly varying thickness in the radial direction, whose geometries are represented by $b/L = 3/7$ and $h_o/h_i = 0{\cdot}2$, $0{\cdot}4$, $0{\cdot}6$, and $0{\cdot}8$, with Poisson's ratio 0·3. It should be noticed that they did not give any information about the ratio of the plate thickness to boundary radii because their analysis was based upon the 2-D thin plate theory, so that h_m/L is assumed to be 0·05 for the present comparison. In the table, there are three frequencies for each annular plate obtained from the 3-D Ritz method (3DR) and the 2-D Ritz method (2DR) [35], which correspond to three circumferential, flexural modes for $n = 0$ (axisymmetric), 1, and 2. The percent different is given by

$$\text{Difference } (\%) = (3\text{DR} - 2\text{DR})/3\text{DR} \times 100. \tag{20}$$

It is observed from the table that the 3-D Ritz method yields lower frequencies than the 2-D Ritz results in the fundamental (lowest) frequencies (occurring for $n = 2$) irrespective of the taper ratios, as expected. For the frequencies of $n = 0$ and 1, as the thickness variation becomes smaller (i.e., the taper ratio h_o/h_i increases), the absolute difference (%) between 2DR and 3DR becomes smaller and then the 3DR results become smaller than the 2DR results. The maximum difference (7·97%) occurs for $n = 0$ (axisymmetric mode) when $h_o/h_i = 0{\cdot}2$. The positive percent differences are unexpected, because an accurate 3-D analysis

TABLE 6

Comparison of frequencies in $2(\omega a^2/h_o)\sqrt{\rho/E}$ from the 3-D and the 2-D theories of completely free, annular plates having linearly varying thickness along the radial direction for $b/L = 3/7$, $h_m/L = 0{\cdot}05$ and $\nu = 0{\cdot}3$

		h_o/h_i			
n	Method	0·2	0·4	0·6	0·8
0(A)	3DR	4·39	4·35	4·49	4·73
	2DR	4·04	4·22	4·45	4·73
	Difference (%)	(7·97)	(2·99)	(0·89)	(0)
1	3DR	8·58	9·02	9·60	10·22
	2DR	8·22	9·03	9·74	10·41
	Difference (%)	(4·20)	(−0·11)	(−1·46)	(−1·86)
2	3DR	2·50	2·47	2·56	2·73
	2DR	2·54	2·49	2·58	2·75
	Difference (%)	(−1·60)	(−0·81)	(−0·78)	(−0·73)

Notes: 3DR ~ the 3-D frequencies by the Ritz method; 2DR ~ the 2-D frequencies by the Ritz method; values in parentheses are the percent difference between 3DR and 2DR.

should typically yield lower frequencies than those from 2-D thin plate theory, mainly because shear deformation and rotary inertia effects are accounted for in a 3-D analysis, but not in 2-D, thin plate theory.

6. CONCLUDING REMARKS

Extensive and accurate frequency data determined by the three-dimensional Ritz analysis have been presented for thick, linearly tapered, annular plates. The analysis uses the three-dimensional equations of the theory of elasticity in their general forms for isotropic materials. They are only limited to small strains. No other constraints are placed upon the displacements. This is in stark contrast with the classical two-dimensional plate theories, which make very limiting assumptions about the displacement variation through the plate thickness.

The method is straightforward, but it is capable of determining frequencies and mode shapes as close to the exact ones as desired. It can therefore obtain benchmark results against which 3-D finite element results may be compared to determine the accuracy of the latter. Moreover, the frequency determinants required by the present method are at least an order of magnitude smaller than those needed by a finite element analysis of comparable accuracy.

REFERENCES

1. R. D. Mindlin 1951 *ASME Journal of Applied Mechanics* **18**, 31–38. Influence of rotatory inertia and shear on flexural motions of isotropic, elastic plates.
2. O. K. Aksentian and T. N. Selezneva 1976 *PMM Journal of Applied Mathematics and Mechanics* **40**, 96–103. Determination of frequencies of natural vibrations of circular plates.
3. Z. Celep 1978 *Ingenieur-Archiv* **47**, 411–420. On the axially symmetric vibration of thick circular plates.
4. Z. Celep 1980 *Journal of Sound and Vibration* **70**, 379–388. Free vibration of some circular plates of arbitrary thickness.
5. A. P. Gupta and N. Mishra 1980 *Journal of Engineering Mathematics* **14**, 101–106. Effect of secondary terms on axisymmetric vibration of circular plates.
6. J. R. Hutchinson 1979 *ASME Journal of Applied Mechanics* **46**, 139–144. Axisymmetric flexural vibrations of a thick free circular plate.
7. K. T. S. R. Iyengar and P. V. Raman 1978 *Journal of the Acoustical Society of America* **64**, 1088–1092. Free vibration of circular plates of arbitrary thickness.
8. G. L. Komissarova 1979 *Soviet Applied Mechanics* **14**, 735–739. Vibrations of a rigidly clamped circular plate.
9. J. So and A. W. Leissa 1998 *Journal of Sound and Vibration* **209,** 15–41. Three-dimensional vibrations of thick circular and annular plates.
10. A. W. Leissa 1969 *Vibration of Plates*, *NASA SP* 160; U.S. Govt. Printing Office; reprinted by the Acoustical Society of America.
11. A. W. Leissa 1978 *The Shock and Vibration Digest* **10**, 21–35. Recent Research in Plate Vibration, 1973–1976: Complicating Effects.
12. A. W. Leissa 1981 *The Shock and Vibration Digest* **13**, 19–36. Plate Vibration Research, 1976–1980: Complicating Effects.
13. A. W. Leissa 1987 *The Shock and Vibration Digest* **19**, 10–24. Recent Studies in Plate Vibrations, 1981–1985: Part II Complicating Effects.

14. H. D. CONWAY 1957 *Zeitschrift für angewandte Mathematik und Mechanik* **37**, 406–407. An analogy between the flexural vibrations of a cone and a disc of linearly varying thickness.
15. H. D. CONWAY 1958 *Ingenieur Archiv* **26**. Some special solutions for the flexural vibrations of disc of varying thickness.
16. A. D. KOVALENKO 1959 *Circular Variable-Thickness Plates*. Moscow: Fitzmatgiz. (In Russian)
17. G. E. KAZANTSEVA 1958 *Prikladnaya Mekhanika* **4**, 197–204. On the vibrations of circular plates of variable thickness. (In Russian)
18. F. F. EHRICH 1956 *Journal of Applied Mechanics* **23**, 109–115. A matrix solution for the vibration modes of nonuniform disks.
19. S. R. SONI and C. L. AMBA RAO 1975 *Journal of Sound and Vibration* **42**, 57–63. On radially symmetric vibrations of orthotropic non-uniform disks including shear deformation.
20. T. IRIE, G. YAMADA and S. AOMURA 1979 *Journal of Sound and Vibration* **66**, 187–197. Free vibrations of a Mindlin annular plate of varying thickness.
21. U. S. GUPTA and R. LAL 1985 *Journal of Sound and Vibration* **98**, 565–573. Axisymmetric vibrations of polar orthotropic Mindlin annular plates of variable thickness.
22. B. SINGH and R. GOEL 1985 *Proceedings of the Workshop on Solid Mechanics, University of Roorkee*, 13–16. Transverse vibrations of an elliptic plate with variable thickness.
23. B. SINGH and D. K. TYAGI 1985 *Journal of Sound and Vibration* **99**, 379–391. Transverse vibration of an elliptic plate with variable thickness.
24. B. SINGH and S. CHAKRAVERTY 1991 *Indian Journal of Pure and Applied Mathematics* **22**, 787–803. Transverse vibration of circular and elliptic plates with variable thickness.
25. B. SINGH and S. CHAKRAVERTY 1992 *Applied Mathematical Modellings* **16**, 269–274. Transverse vibration of circular and elliptic plates with quadratically varying thickness.
26. B. SINGH and S. CHAKRAVERTY 1991 *International Journal of Mechanical Sciences* **33**, 741–751. Transverse vibration of completely free elliptic and circular plates using orthogonal polynomials in the Rayleigh–Ritz method.
27. B. SINGH and S. CHAKRAVERTY 1992 *International Journal of Computers and Structures* **43**, 439–443. On the use of orthogonal polynomial in the Rayleigh–Ritz method for the study of transverse vibration of elliptic plates.
28. B. SINGH and S. CHAKRAVERTY 1992 *Journal of Sound and Vibration* **152**, 149–155. Transverse vibration of simply supported elliptical and circular plates using boundary characteristic orthogonal polynomials in two variables.
29. B. SINGH and S. CHAKRAVERTY 1994 *Journal of Sound and Vibration* **173**, 289–299. Use of characteristic orthogonal polynomials in two dimensions for the transverse vibration of elliptical and circular plates with variable thickness.
30. B. SINGH and V. SAXENA 1995 *Journal of Sound and Vibration* **179**, 879–897. Axisymmetric vibration of a circular plate with double linear variable thickness.
31. R. H. GUTIERREZ, E. ROMANELLI and P. A. A. LAURA 1996 *Journal of Sound and Vibration* **195**, 391–399. Vibrations and elastic stability of thin circular plates with variable profile.
32. J. H. KANG 1997 *Ph.D. Dissertation, The Ohio State University*. Three-dimensional vibration analysis of thick shells of revolution with arbitrary curvature and variable thickness.
33. L. V. KANTOROVICH and V. I. KRYLOV 1958 *Approximate Methods in Higher Analysis*, Groningen: Noordhoff.
34. J. SO and A. W. LEISSA 1997 *Journal of Vibration and Acoustics* **119**, 89–95. Free vibrations of thick hollow circular cylinders from three-dimensional analysis.
35. G. K. RAMAIAH and K. VIJAYKUMAR 1975 *Journal of Sound and Vibration* **40**, 293–298. Vibrations of annular plates with linear thickness profiles.